Electronic Supplementary Material (ESI) for Journal of Materials Chemistry B.

Supporting Information

Controlling integrin-based adhesion to a degradable electrospun fibre scaffold via SI-ATRP

By *Andrew E. Rodda,* Francesca Ercole, Veronica Glattauer, David R. Nisbet, Kevin E. Healy, Andrew P. Dove, Laurence Meagher* and *John S. Forsythe **

Materials and methods

Instrumental Methods

NMR

^{1}H NMR spectra were recorded on a Bruker DPX-400, AC-400, or DRX-500 spectrometer at 298 K. Chemical shifts are reported in parts per million (ppm) and referenced to the chemical shift of the residual solvent resonances ($CHCl_3$: ^{1}H δ = 7.26 ppm).

GPC

Gel permeation chromatography (GPC) studies of the Br-PCL macroinitiator was conducted on a system composed of a Varian 390-LC Multi detector suite fitted with differential refractive index, light scattering, and ultraviolet detectors equipped with a guard column (Varian Polymer Laboratories PLGel 5 μM, 50 × 7.5 mm) and two mixed D columns (Varian Polymer Laboratories PLGel 5μM, 300 × 7.5 mm). The mobile phase was $CHCl_3$ (HPLC grade) with 0.5 % TEA, at a flow rate of 1.0 mL min^{-1}. Samples were filtered prior to analysis (0.45 μm) and results were calibrated against Varian Polymer Laboratories Easi-Vials linear polystyrene standards (162 - 2.4 × 10^{5} g mol^{-1}) using Cirrus v3.3 software. Polymer solutions were filtered through 0.45 μm filters before injection.

GPC analyses of the degraded fibre samples were performed using a Shimadzu modular system comprising a DGU-20A3R degasser unit, an SIL-20A HT autosampler, a 10.0 μm bead-size Agilent PLgel guard column (50 × 7.8 mm) followed by three Agilent PLgel Mixed C columns (300 × 8 mm, bead size: 5 μm), a SPD-20A UV/Vis detector, and an RID-10A differential refractive-index detector. The temperature of columns was maintained at 40°C

using a CTO-20A oven. The eluent was tetrahydrofuran (Chromasolv Plus for HPLC) and the flow rate was kept at 0.8 mL/min using a LC-20AD pump. A molecular weight calibration curve was produced using commercial narrow molecular weight distribution polystyrene standards with molecular weights ranging from 500 to 2×10^6 g/mol. Polymer solutions at approx. 2 mg/mL were prepared and filtered through 0.45 μm PTFE filters before injection.

XPS

XPS analysis was performed using an AXIS Ultra DLD spectrometer (Kratos Analytical Inc., Manchester, UK) with a monochromated Al K□ source at a power of 150 W (15 kV × 10 mA), a hemispherical analyser operating in the fixed analyser transmission mode and the standard aperture (analysis area: 0.3 mm × 0.7 mm) The total pressure in the main vacuum chamber during analysis was typically between 10^{-9} and 10^{-8} mbar. Charging of the samples during irradiation was reduced by the use of an internal flood gun, coupled with a magnetic immersion lens. Fibrous samples were also mounted beneath a metallic mask to further reduce problematic charging of the sample. Survey spectra were acquired at a pass energy of 160 eV, while high resolution C 1s spectra were recorded at 20 eV pass energy. Each specimen was analysed at an emission angle of 0° as measured from the surface normal. Under these conditions the XPS analysis depth typically ranges between 5 and 10 nm depending on the element.

Data processing was performed using CasaXPS processing software version 2.3.15 (Casa Software Ltd., Teignmouth, UK). Curve fitting was performed using a simplex algorithm where residuals were minimised with multiple iterations. Binding energies were referenced to

the aliphatic hydrocarbon peak at 285.0 eV. Peaks resulting from primary and secondary ester carbons were constrained to have identical integral and shape parameters.

DSC

Differential scanning calorimetry was performed using a Pyris 1 calorimeter. Two heating cycles were performed between -50 °C and 150 °C, using a heating rate of 5 °C/min. The analysis result obtained with the second temperature cycle were reported.

SEM

Electrospun fibre samples were dried under vacuum and attached to a stub using double-sided carbon tape. Samples were then coated with a thin layer of gold using a sputter coater (Ulvac VPS-020) at 4 mA for 3 minutes. Images were obtained using a benchtop SEM (FEI Phenom, 5 kV) according to manufacturer instructions.

Supplementary experimental methods and results

Characterisation of Br-PCL macroinitiator

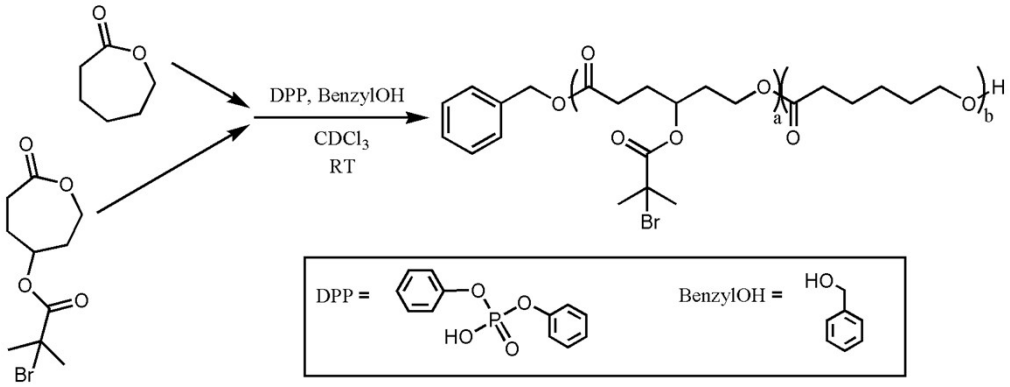

Scheme S1: Polymerisation of Br-PCL macroinitiator

The polymer was produced by adapting the protocol reported by Ercole et al., [1] using toluene as the bulk solvent (**Scheme S1**). The ratio of $[Monomers]_0$:$[Initiator]_0$:[DPP Ligand] was 500:1:10, with an increased polymerisation time (compared to the previous work) of 24 hours compared to 14.5 hours. Characterisation of composition, molecular weight and dispersity is reported in **Table S2**. While the PCL aminolysis/hydrolysis approaches to introducing surface functional groups, i.e. the ATRP initiating group, can result in the degradation of of the PCL backbone (which in turn causes surface erosion of the PCL fibres),[2-4] the polymerisation of a functional PCL-based monomer allows for ready modification of the fibre surface properties without adversely affecting the degradable polymer core.

Table S1: Analysis of Br-PCL macroinitiator polymer used in this study. A similar previously-described, lower molecular weight copolymer is shown for comparison.

Polymer	% Br-CL (feed) [a]	% conv. (CL/Br-CL) [b]	Final % Br-CL [c]	$M_{n\ theo.}$ (kDa) [d]	M_n (GPC/NMR) (kDa) [e][f]	Đ [f]
Br-PCL	15	82/91	14	61.4	91.6/77.3	1.24
Br-PCL (Ercole et al.) [1]	16	61/63	13	40.5	65.9/50.0	1.07

[a] Molar percentage of Br-CL in feed. [b] Calculated from ratio of integrals (^{1}H NMR) of monomer peaks to broad polymer peaks in the crude polymerization mixture. [c] Composition of purified polymer calculated from ^{1}H NMR [d] M_n (theo.) was determined from the feed concentrations of the monomers (Br-CL and ε-CL) and initiator (I) and their final conversions (as determined by comparing monomer and polymer peaks) using the equation: M_n (theo.) = (([Br-CL]/$[I]_0$) × conversion × (MW of Br-CL)) + (([ε-CL]/$[I]_0$) × conversion × (MW of ε-CL)) + (MW of initiator) [e] M_n was determined from ^{1}H NMR by integrating the peaks related to the aromatic end groups and comparing to those of the polymer. [f] Determined by GPC analysis in $CHCl_3$ with 0.5 vol% triethylamine, using polystyrene standards.

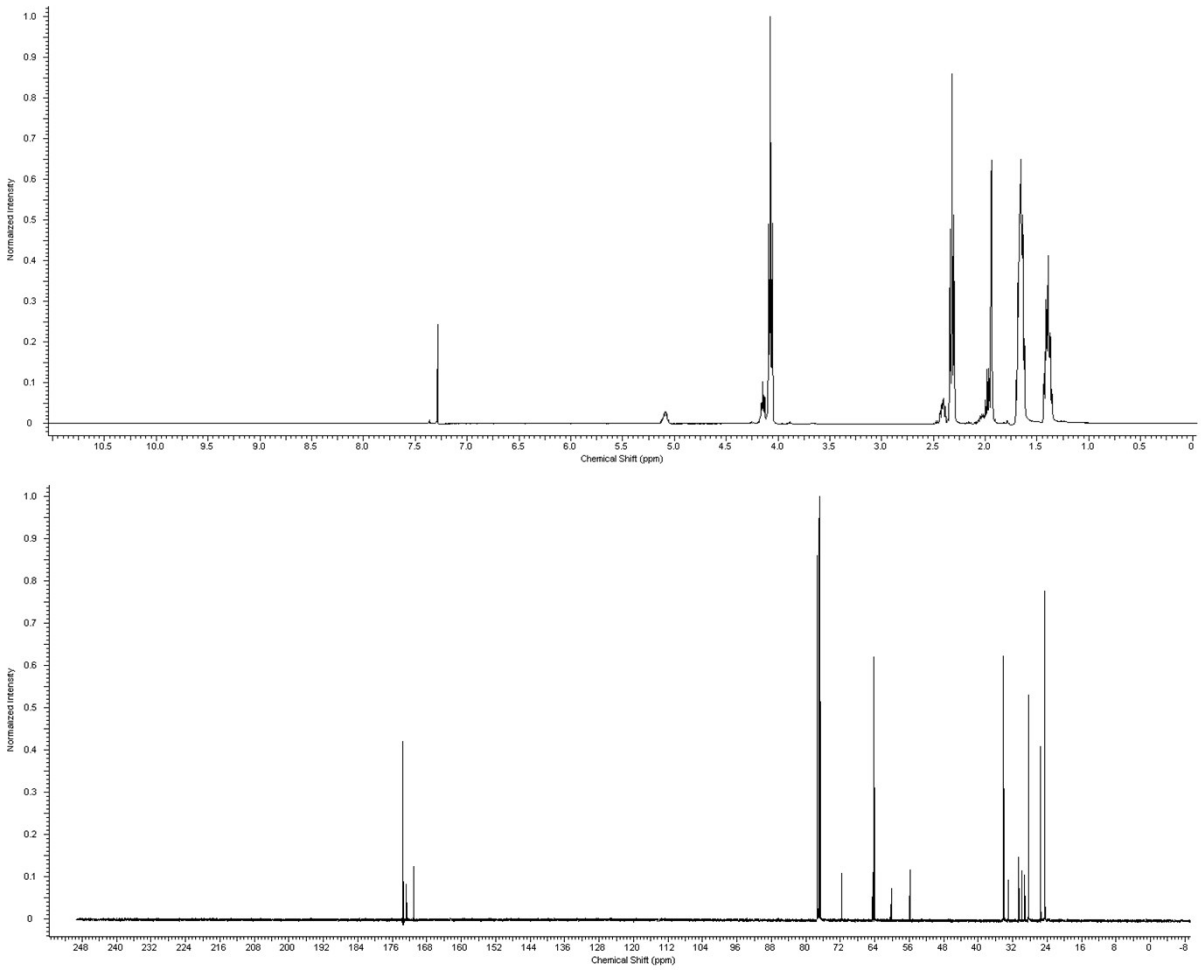

Figure S1: ^{1}H (top) and ^{13}C (bottom) NMR spectra for the Br-PCL macroinitiator used in this study.

Electrospinning of Br-PCL blends

Methods

Four separate polymer solutions were prepared, comprising 14 %, 25 %, 50 % and 75 % blends of Br-PCL with commercially-obtained pure PCL, using 3:1 chloroform:methanol as the solvent. Total polymer concentration was adjusted empirically to produce solutions of similar viscosity; while Br-PCL was of a similar M_n to the commercial PCL, a lower degree of polymerisation and small amounts of branching meant that chain entanglement concentration and viscosity were decreased for a similar mass concentration. Quantities that were disolved in 2 ml of solvent are shown in **Table S2.**

Table S2: Solutions used to investigate electrospinning of Br-PCL/PCL blends

	14 %	**25 %**	**50 %**	**75 %**
Br-PCL	36 mg	71 mg	150 mg	370 mg
PCL	216 mg	213 mg	150 mg	123 mg

These solutions were electrospun on a custom-built electrospinner using the following conditions: +15 kV (18 gauge needle), 0 kV (plate collector covered with aluminium foil), 0.6 ml/hr, 22 °C, 42 % relative humidity. Fibre matrices were spun from working distances of 10, 14, 18 and 22 cm and stored in a vacuum desiccator prior to analysis. Similar sets of fibres were electrospun by reversing the polarities of the needle and collector.

Results

Samples of electrospun fibres were analysed using XPS to determine the relative surface bromine content of the electrospun fibres. A series of fibres was also produced using a

reversed polarity electrospinning setup (i.e. a negatively charged needle and positively charged collector) to check for charge-driven phase separation of the blended polymers. Surface bromine abundance consistently increased along with Br-PCL content, but no consistent trend in bromine concentration was observed for fibres produced via changed polarity (**Figure S2A**). This is in contrast to a recent report of PCL that was end-functionalised with similar ATRP initiator groups.[5] When compared to the atomic composition predicted via the stoichiometry of the polymer blend, the measured atomic abundance of Br was lower than expected in all spectra, which we attributed either to adventitious carbon contamination, or potentially to loss of Br during analysis as a result of X-ray damage to the sample.

While solutions with high percentages of Br-PCL produced scaffolds with higher surface concentrations of bromine, they were also more likely to form fibres with a "liquified" morphology (**Figure S2(B-I)**). Working distance was also found to have a secondary influence on fibre morphology, with larger working distance reducing the observed extent of the liquified morphology, potentially by allowing greater time for solvent evaporation prior to deposition. Unlike solutions that were blended with PCL, solutions of neat Br-PCL did not produce fibres under these conditions, nor through a range of alternative electrospinning protocols. We suggest that this can be explained by supposing that the ATRP initiating group alters the packing of the PCL crystals, and thereby prevents the effective solidification of the Br-PCL fibres. As can be observed in **Figure S3**, analysis of the melting temperature of Br-PCL via differential scanning calorimetry (DSC) showed that Br-PCL melted at a far lower temperature (30 – 35 °C) than PCL, indicating that the polymer packing had been disrupted by the addition of the ATRP initiator group. However, examination of the fibres used in later experiments (1:3 blend of Br-PCL:PCL) showed good miscibility and a melting temperature similar to that of PCL (approximately 55 °C).

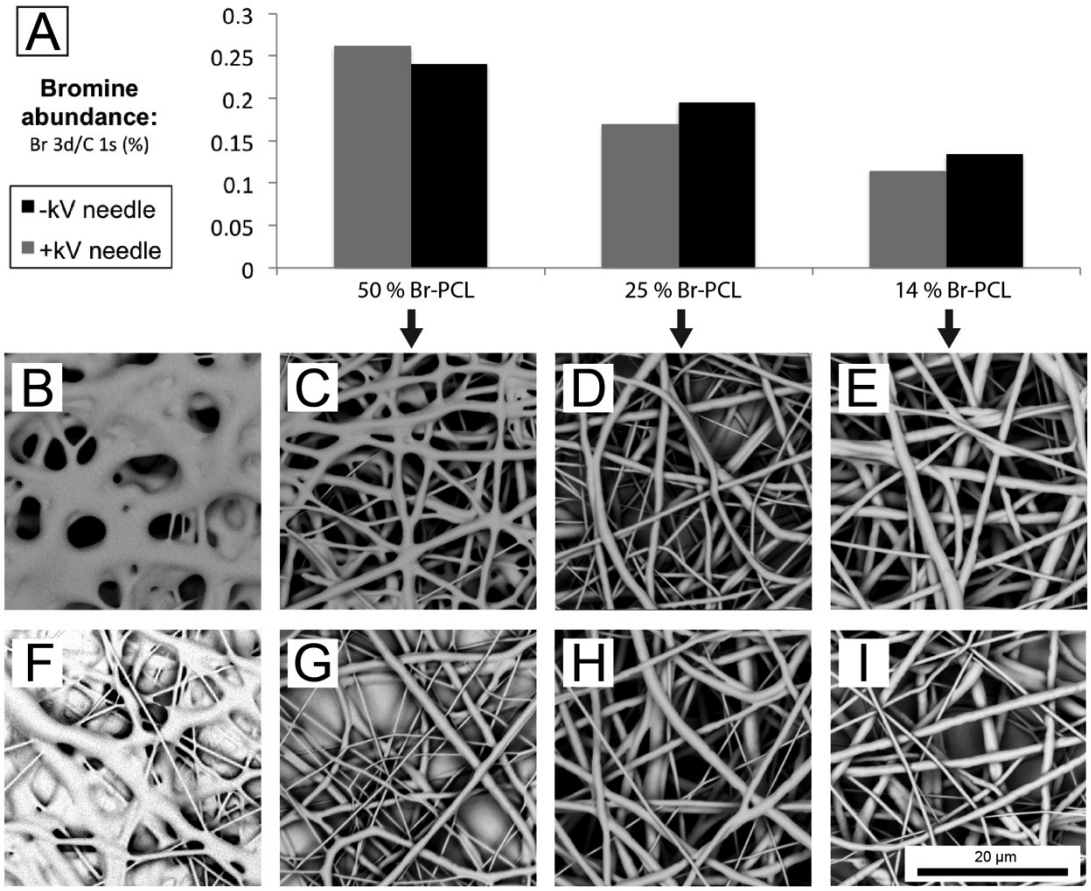

Figure S2: Electrospinning of Br-PCL:PCL blends. (A) Bromine abundance at the surface of fibrous samples produced using both positively and negatively-charged jets, as determined via XPS. (B-E) 10 cm working distance (F-I) 22 cm working distance. (B,F) 75 % blend of Br-PCL:PCL. (C,G) 50 % blend. (D,H) 25 % blend. (E,I) 14 % blend. All images are of fibres produced using a positively charged jet; those produced with a negatively charged jet showed identical morphology.

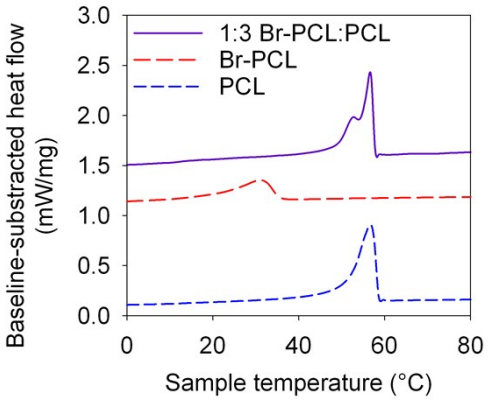

Figure S3: DSC analysis of Br-PCL shown a reduced melting temperature compared to commercial PCL. However, a 1:3 blend of Br-PCL:PCL retained a higher melting temperature. The top two curves have been offset vertically from baseline readings that match those of PCL.

KF deprotection

Treatment with a 0.5 M solution of KF in methanol successfully removed silyl protecting groups from the brush layers, as determined by XPS analysis of silicon abundance. However, analysis of the deprotected fibres showed that the integrity of the grafted polymer brush coating was compromised by longer reaction times. A decrease in the ether carbon:hydrocarbon ratio was observed following treatment with KF, along with traces of bromine. Br-PCL in solutions of chloroform/methanol (from electrospinning) had also been observed to degrade (yellowed solution and small extra resonance detected by NMR at 3.67 ppm) which we ascribe to transesterification of the Br-PCL by methanol. We thus believe that the methanol/KF solution degraded the coatings via this same reaction, leading to release of the grafted brushes and exposure of the underlying electrospun fibres.

As can be seen in **Table S3**, deprotection for 6 hours resulted in noticeably less hydrocarbon species being present in the spectra compared to a 24 hour treatment, and a concomitant increase in the abundance of ether carbon. As might be expected from a theoretical deprotection reaction with no side reactions, hydrocarbon content decreased following reaction with KF for 6 hours, due to the removal of the trimethylsilyl protective group. Furthermore, XPS analysis indicated that the shorter reaction time removed a similar quantity of silicon from the surfaces as a longer reaction. While it is likely that the transesterification reaction is still occurring to a small degree (see **Table S3**), a 6 hour deprotection time was adopted as the standard for grafted Br-PCL fibres in further experiments.

Table S3: XPS atomic abundance on fibre samples following deprotection using 0.5 M KF. Data are reported as mean atomic % (standard deviation). Shortened reaction times led to higher abundances of oxygen and ether carbon and lower abundances of hydrocarbons and bromine (indicating better retention of the brush coating) while the silyl protecting group was removed equally well (reduction in Si 2p).

Peak (approximate position)		**Prior to KF treatment**	**KF 6 hrs**	**KF 24 hrs**
O 1s (529 eV)		27 (0)	28 (0)	26 (0)
C 1s		72 (0)	72 (0)	73 (0)
	Hydrocarbon (285 eV)	15 (1)	12 (3)	19 (3)
	Ether (286.4 eV)	46 (2)	43 (2)	37 (2)
	Ester/Secondary Ester (289.1/285.7 eV)	6 (0)	9 (2)	8 (0)
Si 2p (100 eV)		0.7 (0.1)	0.2 (0.0)	0.3 (0.1)
Br 3d (69 eV)		0.00	0.03 (0.01)	0.05 (0.01)

Grafting of TMS-Prg-HEGMA from solutions containing varied concentrations of monomer

Grafting was performed as described above, using either 10 %, 20 % or 30 % molar concentration TMS-Prg-HEGMA (with regard to total monomer). The abundance of silicon on the surfaces of the grafted fibres was found to increase along with the feed concentration of alkyne monomer (**Table S4**), although the detected abundances are higher than would be predicted based on the stoichiometry of the feed solution. This is in accordance with previous observations for this monomer,[6] and is supported by the modelling work below, which suggests that TMS-Prg-HEGMA is preferentially incorporated into the polymer brush coating, and shows that the density of surface reactive groups can be easily manipulated.

Table S4: XPS atomic abundance on the surfaces of Br-PCL-graft-poly(TMS-Prg-HEGMA-co-OEGMA) using 10 %, 20 % and 30 % TMS-Prg-HEGMA monomer solutions. The abundance of silicon on the surfaces increases with the proportion of alkyne monomer in the feed. Determined via XPS analysis of single samples Data are reported as total atomic percent.

Peak		**10 % alkyne**	**20 % alkyne**	**30 % alkyne**
C 1s		71.6	72.0	71.1
	Hydrocarbon (285 eV)	21	23	21
	Ether (286.4 eV)	37	34	35
	Ester/Secondary Ester (289.1/285.7 eV)	7	7	7
O 1s (529 eV)		26.9	26.0	26.5
Si 2p (100 eV)		1.4	1.7	2.2

Semi-quantitative analysis of fluorine content in p(OEGMA-co-Prg-HEGMA) brush coatings, derivatised via click reaction with TFAB

The atomic compositions of the graft layer were modelled in a speadsheet using the following vectors, and fitted to survey spectra (examples of survey spectra can be seen in **Figure S4**).

Atom	**X_1 = TMS-Prg-HEGMA**	**X_2 = Prg-HEGMA**	**X_3 = OEGMA 475**	**X_4 = TFAB**
F	0	0	0	3
O	8	8	11	2
N	0	0	0	3
C	22	19	23	10
Si	1	0	0	0

And the total composition was modelled as:

$$\bar{X} = R_g X_3 + (1 - R_g)\left[Y_d(X_2 + Y_c X_4) + (1 - Y_d)X_1\right]$$

Where: R_g = Graft ratio (% OEGMA vs total monomer)

Y_d = Yield of deprotection reaction

Y_c = Yield of click reaction

Errors were defined as:

$$\delta_i = \frac{X_i - \bar{X}_i}{\bar{X}_i}$$

Normalisation was used to compensate for the widely varied abundances of different elements, but equal importance in fitting the model. The entire process was also repeated, with similar results, for errors that were normalised to the experimental measurements rather than the model predictions.

The sum of squared errors was minimised by optimising the three parameters ($R_g/Y_d/Y_c$) until a minimum was reached that was stable for perturbations in all three parameters.

This technique makes several approximations, which prevent it from being fully quantitative: it assumes no contamination by either adventitious carbon or silicon, both of which were commonly observed in Br-PCL polymer-based coatings. It also assumes that no signal is detected from the underlying macroinitiator polymer.

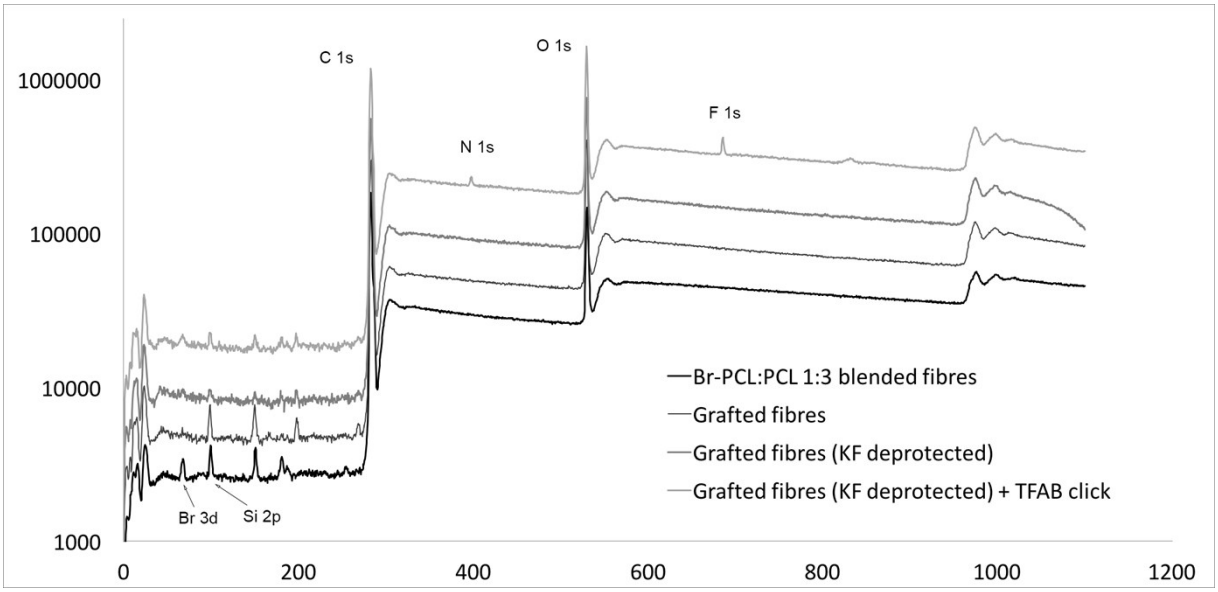

Figure S4: Survey spectra of fibres at various stages during functionalisation

Degradation behaviour of grafted and non-grafted fibres

Grafted and non-grafted fibre samples were exposed to a phosphate buffered saline (PBS) solution for 21 days in order to examine their degradation behaviour. We were interested in determining whether the presence of hydrophilic brushes on the fibre surface would affect the degradation profile of the polymers. In particular, it was hypothesised that the increased wetting at the surface might increase the rate of degradation, via hydrolysis of esters within either the PCL backbone or the grafted brushes, making the fibre structure unstable. Samples were examined by GPC and XPS, both before and after exposure.

No noticeable degradation was observed in either of the sample sets up to 21 days. These combined results indicate that the grafted fibres were stable for relatively long periods of time under these conditions, in a similar manner to unmodified PCL fibres, which are known to degrade over a period of up to several years.[7] A bimodal peak was observed for all samples, with the low MW peak being attributed to non-grafted Br-PCL, while the higher, broader MW peak was most likely due to a combination of both grafted Br-PCL and PCL. The commercial PCL used had a similar molecular weight to the Br-PCL but a higher degree of polymerisation, and thus was detected earlier than Br-PCL during GPC of the individual polymers. As would be expected, this higher MW peak was relatively larger in grafted samples than in non-grafted ones due to the presence of grafted Br-PCL chains. The presence of non-grafted Br-PCL chains within the grafted samples is consistent with the earlier XPS results that showed minimal surface enrichment of the bromine moiety during electrospinning (i.e. Br-PCL is evenly distributed throughout the interior of the fibre).

Further studies of the surface coating with XPS also showed no significant change in the composition of grafted/non-grafted fibre surfaces following exposure to PBS, demonstrating

that the surface coating was intact at this timepoint. This is in contrast to grafted samples that were exposed to KF/methanol deprotection solution for 16 or 24 hours; in this case, a decrease in the abundance of ether carbon was clearly observed, signifying a loss of ethylene glycol chains from the surface.

Our previous study of similar brush coatings on non-degradable polystyrene-based fibres did not observe a significant decrease in ether carbon on exposure to KF/methanol for extended time periods. This indicated that the loss of ether carbon seen here is most likely through hydrolysis of Br-PCL molecules, rather than of the grafted polymer brushes themselves. The scission of the Br-PCL chains within the electrospun fibres was then responsible for the release of grafted brushes from the surface. [6]

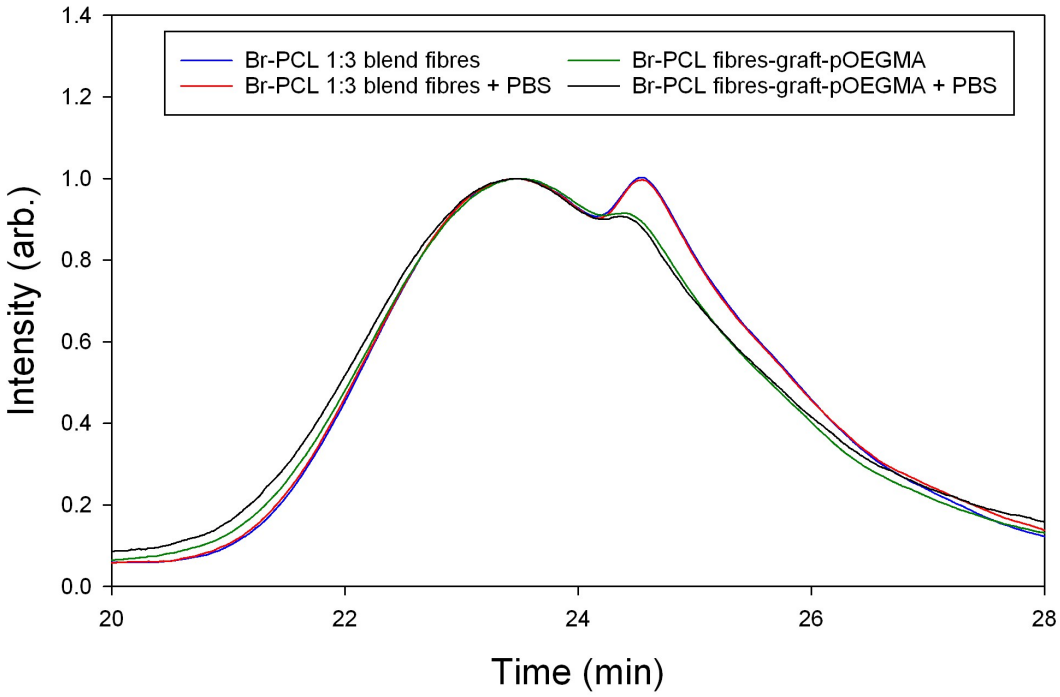

Figure S5: GPC traces of grafted and non-grafted fibre samples, both with and without 21 day exposure to PBS solution to quantify degradation of the scaffold via hydrolysis. No noticeable difference was seen between samples before and after exposure for either sample

type. Individual analysis of PCL and Br-PCL produced curves that appeared to correspond to the two major peaks observed here.

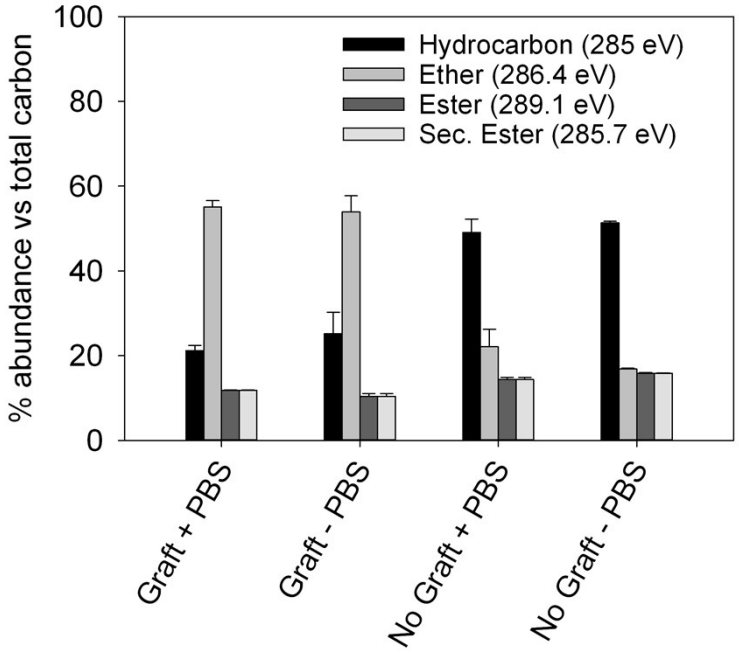

Figure S6: Peak fitting quantification of high resolution C 1s XPS spectra of grafted and non-grafted fibres with/without exposure to PBS solution for 21 days. No significant changes were seen following PBS exposure, indicating that the fibre coatings were stable.

L929 fibroblast culture: automated cell shape analysis

Methods:

Scaffolds were prepared as for MSC cultures. Stock cultures of L929 murine fibroblasts (cell line ATCC-CCL-1, Rockville, MD, USA) were cultured in minimum essential medium containing 10 % fetal bovine serum (FBS) and 1 % nonessential amino acids. L929 cells were washed with PBS and harvested with TrypLE™ Express (Gibco), then washed twice in media. They were then seeded onto fibre scaffolds at a density of 2.5×10^4 cells/cm^2 (relative to the area of the underlying plate) and incubated for 24 hours. Cells were then stained and imaged as described for MSCs.

Images of L929 cells taken at low magnification were processed using brightness/contrast, automated edge-finding and thresholding to create a black and white image, which was analyzed using ImageJ Particle Analysis tool. Cells at the edge of the image and clusters of multiple cells were excluded from analysis. Several hundred cells were analyzed for both conditions and the resulting shape parameters for cells on the two surfaces were compared using a Mann-Whitney non-parametric test performed using Prism 6 software.

Cells grown on fibres with attached cRGD were spread, while those grown on brush-only surfaces were far more rounded. Analysis of the results showed a significant change in the shape of fibroblasts cultured on the two surfaces (**Figure S7**).

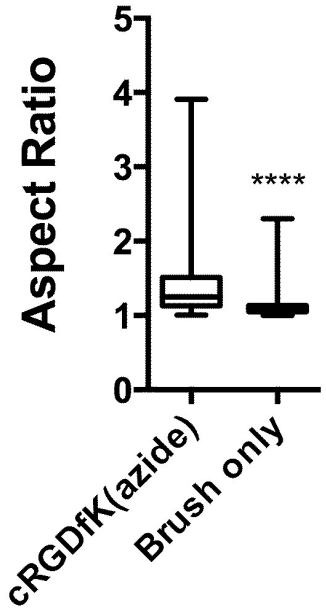

Figure S7: L929 fibroblast cells had significantly higher aspect ratios ($p < 0.0001$) when cultured on fibrous substrates bearing the cRGDfK(azide) peptide, compared to brush-only controls.

MSC cultures: low magnification images

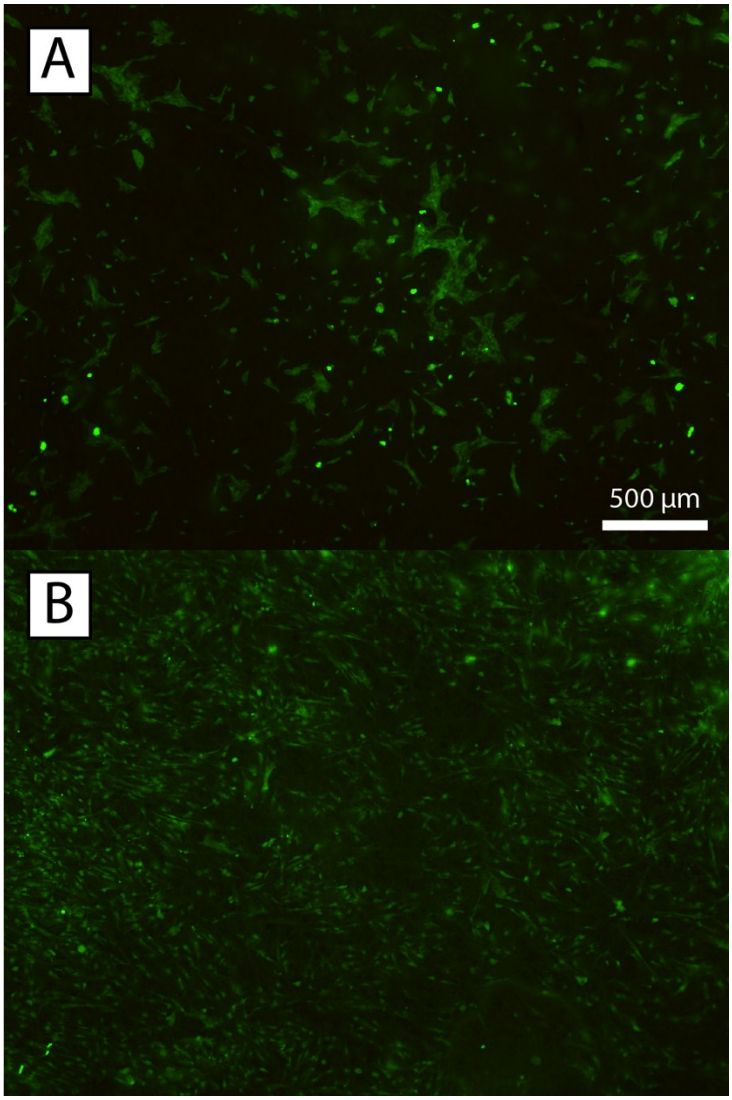

Figure S8: Wide angle images of MSCs cultured in FBS-containing medium on fibres with brushes only (top) and cRGD functionalised brushes (bottom).

1. Ercole, F.; Rodda, A. E.; Meagher, L.; Forsythe, J. S.; Dove, A., Surface Grafted Poly(E-Caprolactone) Prepared Using Organocatalysed Ring-Opening Polymerisation Followed by Si-Atrp. *Polym. Chem.* **2014,** *5*, 2809-2815.
2. Jiang, H.; Wang, X.; Li, C.; Li, J.; Xu, F.; Mao, C.; Yang, W.; Shen, J., Improvement of Hemocompatibility of Polycaprolactone Film Surfaces with Zwitterionic Polymer Brushes. *Langmuir* **2011,** *27*, 11575-11581.
3. Xu, F.; Wang, Z.; Yang, W., Surface Functionalization of Polycaprolactone Films Via Surface-Initiated Atom Transfer Radical Polymerization for Covalently Coupling Cell-Adhesive Biomolecules. *Biomaterials* **2010,** *31* (12), 3139-3147.
4. Yuan, W.; Li, C.; Zhao, C.; Sui, C.; Yang, W.-T.; Xu, F.-J.; Ma, J., Facilitation of Gene Transfection and Cell Adhesion by Gelatin-Functionalized Pcl Film Surfaces. *Adv. Funct. Mater.* **2012,** *22*, 1842-1851.
5. Harrison, R. H.; Steele, J. A. M.; Chapman, R.; Gormley, A. J.; Chow, L. W.; Mahat, M. M.; Podhorska, L.; Palgrave, R. G.; Payne, D. J.; Hettiaratchy, S. P.; Dunlop, I. E.; Stevens, M. M., Modular and Versatile Spatial Functionalization of Tissue Engineering Scaffolds through Fiber-Initiated Controlled Radical Polymerization. *Adv. Funct. Mater.* **2015,** *25* (36), 5748-5757.
6. Rodda, A. E.; Ercole, F.; Glattauer, V.; Gardiner, J.; Nisbet, D. R.; Healy, K. E.; Forsythe, J. S.; Meagher, L., Low Fouling Electrospun Scaffolds with Clicked Bioactive Peptides for Specific Cell Attachment. *Biomacromolecules* **2015,** *16* (7), 2109-2118.
7. Cipitria, A.; Skelton, A.; Dargaville, T. R.; Dalton, P. D.; Hutmacher, D. W., Design, Fabrication and Characterization of Pcl Electrospun Scaffolds: A Review. *J. Mater. Chem.* **2011,** *21*, 9419-9453.